Journal of the Indian Society of Remote Sensing (December 2018) 46(12):1925–1937
https://doi.org/10.1007/s12524-018-0846-3

RESEARCH ARTICLE

Assessing Metal-Induced Changes in the Visible and Near-Infrared Spectral Reflectance of Leaves: A Pot Study with Sunflower (*Helianthus annuus* L.)

Paresh H. Rathod[1,4] · Carsten Brackhage[2] · Ingo Müller[3] · Freek D. Van der Meer[1] · Marleen F. Noomen[1]

Received: 2 July 2016 / Accepted: 23 August 2018 / Published online: 12 October 2018

Abstract
The aim of this study was to monitor changes in leaf spectral reflectance due to phytoaccumulation of trace elements (Cd, Pb, and As) in sunflower mutant (M5 mutant line 38/R4-R6/15-35-190-04-M5) grown in spiked and in situ metal-contaminated potted soils. Reflectance spectra (350–2500 nm) of leaves were collected using portable ASD spectroradiometer, and respective leaves sample were analyzed for total metal contents. The spectral changes were quite noticeable and showed increased visible and decreased NIR reflectance for sunflower grown in soil spiked with 900 mg As kg^{-1}, and in in situ metal-contaminated soils. These changes also involved a *blue-shift* feature of red-edge position in the first derivatives spectra, studied vegetation indices and continuum removed absorption features at 495, 680, 970, 1165, 1435, 1780, and 1925 nm wavelength. Correlograms of leaf-metal concentration and reflectance values show highest degrees of overall correlation for visible, near-infrared, and water-sensitive wavelengths. Partial least square and multiple linear regression statistical models (cross-validated), respectively, based on Savitzky–Golay filter first-order derivative spectra and combination of spectral feature such as vegetation indices and band depths yielded good prediction of leaf-metal concentrations.

Keywords Metal-contaminated soils · Sunflower · Spectral reflectance · Phytoremediation · Visible and near-infrared spectroscopy

Introduction

Looking at the environmental consequences associated with metal-contaminated sites, remediation has become an important task. Many physicochemical methods have been materialized for remediating metal-contaminated sites, and phytoremediation (i.e., cleaning-up process that employs various types of plants to remove, transfer or stabilize metals in the soil) is among the most emphasized eco-friendly and inexpensive method (Cundy et al. 2016; Mench et al. 2010; Pilon-Smits 2005; Vangronsveld et al. 2009). However, like any remediation system, phytoremediation does have shortcomings: (1) there are only few recognized hyperaccumulators, i.e., exceptional plant species, which tolerate as well as accumulate large amounts of metals into plant parts when growing on heavily metal-contaminated soils (Prasad and de Oliveira Freitas 2003), (2) usually, it takes long time (> 10 years) to clean up hazardous contaminated sites when focusing on total concentrations, and (3) prolonged exposure to the elevated soil metal concentration causes severe environmental stress to plants, even to hyperaccumulators (Prasad 2004). Cundy et al. (2015) defined a number of site-based indicators to identify a kind of implementation window, e.g., large areas,

✉ Paresh H. Rathod
rathod23904@aau.in

[1] Department of Earth Systems Analysis, Faculty of Geo-information Science and Earth Observation, University of Twente, 7514AE Enschede, The Netherlands

[2] Institute for General Ecology and Environmental Protection, Technical University, TU Dresden, 01737 Tharandt, Germany

[3] Saxon State Office for Environment, Agriculture and Geology, 09599 Freiberg, Germany

[4] Present Address: Anand Agricultural University, Anand, Gujarat State, India

where contamination may cause concern but is not at strongly elevated level, where biological soil functionality and ecosystem service is required, where there is a need to restore marginal land to produce non-food crops and where there are some budgetary or deployment constraints regarding other remediation options. Although phytoremediation can provide strong benefits in terms of risk management, deployment costs, and sustainability for a range of site problems, awareness and take up in remediation practice is low, at least in a European context (Cundy et al. 2016; Kidd et al. 2015; Onwubuya et al. 2009). The barriers to wider adoption of gentle remediation options (GRO), especially in Europe, arise both from the nature of GRO as remediation techniques, and market and stakeholder perceptions of uncertainties over whether these methods can achieve effective risk management in the long term.

Such long-term and plant-based clean-up processes, therefore, require a technique that can remotely monitor the soil–plant system, and aid in assessing the contamination level in soil and plant. Monitoring spectral reflectance of vegetation growing in metal-contaminated soil could be the one approach to optimize the phytoremediation system (Sridhar et al. 2007a, b). Spectral reflectance signatures from plant in the visible, near-infrared, and short-wave infrared regions have been widely documented to assess the contaminants (Noomen 2007; Rathod et al. 2013 and references therein). A healthy plant has a minimum spectral reflectance in the visible wavelengths resulting from the pigments in leaves, while maximum reflectance in the near infrared due to light scattering by internal structures of leaves. Accordingly, stressed plant can be monitored by significantly lower reflectance in the infrared, higher reflectance in visible wavelengths, and through various vegetation indices calculations (Blackburn 2007).

Unlike some essential metals (Mn, Fe, Cu, and Zn) for plant metabolism, certain metals such as Cd, Pb, and As are toxic to the plant even at rather low concentrations (Cuypers et al. 2009; Prasad 2004). They influence pigment synthesis, structural and ultrastructural changes in plant tissue, and these alterations can be revealed by the spectral signatures (Font et al. 2007; Horler et al. 1980; Sridhar et al. 2007b). With these views, the present study was taken to assess the metal-induced plant stress using spectral reflectance in 350–2500 nm domains and thus to monitor the metal-accumulation into the plant. Sunflower, with moderate metal-accumulation and high biomass production, is a potential candidate for phytoremediation (Adesodun et al. 2010; Herzig et al. 2014; Nehnevajova et al. 2005).

Materials and Methods

Sunflower (*Helianthus annuus*): Pot Experiment Setup

A pot experiment was setup in glass chambers with filtered air circulation and controlled temperature at a test facility (Prüffeld) of Institute of General Ecology, TU Dresden in Tharandt, Germany, from July–Nov 2011. Three different soil substrates from permanent soil monitoring sites of Saxon state were used: (1) S_1: uncontaminated soil substrate (loamy fine sand) from Melpitz, (2) S_2: heavily contaminated grassland soils (sandy loam) from Hilbersdorf, and (3) S_3: severely contaminated floodplains soils (sandy clay loam) from Neuhilbersdorf. Source of metal-contamination both at Hilbersdorf and Neuhilbersdorf is mainly due to abandoned Artisanal mining and emission from a larger ore processing about 1–2 km away at Muldenhütten. Neuhilbersdorf as a floodplain site is additionally affected by stream sediments from the Freiberger Mulde River directly after passing Muldenhütten smelter area. Top soils from these sites were collected and sieved through 0.5 cm using horizontal mechanical sieve.

Using the uncontaminated soil substrate from Melpitz (S_1), in addition metal-contamination was simulated by spiking three metal-salts, viz., cadmium as $Cd(NO_3)_2$·$4H_2O$, lead as $Pb(NO_3)_2$, and arsenic as As_2O_3, individually each at different levels and in mixture at their higher levels (treatment details in Table 1). Metal concentration was raised to higher levels (Cd, 10 and 20; Pb-1200; As, 100 and 900 mg kg^{-1}) to stimulate severe metal-contamination in soils. Spike solutions of Cd and Pb were prepared by sequential dilutions of $Cd(NO_3)_2$·$4H_2O$ and $Pb(NO_3)_2$ in deionized water, while As_2O_3 was dissolved in a NaOH-solution and adjusted to near neutral pH. The prepared metal-spike solutions were then added to the respective bulk of soil of treatments (i.e., 48 kg soil for 4 replicate pots for each treatment; $9 \times 4 = 36$ pots were prepared for 9 treatment sets). The spiked soils were mixed homogenously and kept for two wetting–drying cycles for 10–12 days to equilibrate metal-spiking. Each 40 kg metal-spiked soil was then divided on weight basis (10 kg pot^{-1}), and pots were thereafter randomized between four glass chambers. Initial soil sample was collected from each pot before transplanting sunflower seedlings for the analysis of total metals. Start concentration of metals in soil is given in Table 1.

Sunflower (*Helianthus annuus* L.) was used as a test crop, and seeds of 5th generation mutant inbred line (M5 mutant line 38/R4-R6/15-35-190-04-M5) were obtained from Phytotech Foundation (PT-F), Bern, Switzerland. This inbred line was developed with in mutagenesis and

Table 1 Treatment details and metal concentration after metal-spiking to uncontaminated soil before planting

Details of metal-spiking treatments	Start concentration of metals[a] in soils (in mg kg^{-1})		
	Cadmium	Lead	Arsenic
Metal-spiking to S_1: uncontaminated soil			
S_1-control: no metal-spiking	0.4 (± 0.01)	27.3 (± 1.98)	4.9 (± 0.23)
S_1-Cd_1: 10 mg kg^{-1}	10.5 (± 0.19)	–	–
S_1-Cd_2: 20 mg kg^{-1}	23.1 (± 0.43)	–	–
S_1-Pb_1: 1200 mg kg^{-1}	–	1478 (± 138.7)	–
S_1-As_1: 100 mg kg^{-1}	–	–	94.7 (± 5.72)
S_1-As_2: 900 mg kg^{-1}	–	–	910 (± 66.8)
S_1-Mix: 20 Cd + 1200 Pb + 900 As; mg kg^{-1}	22.0 (± 0.50)	1677 (± 77.1)	980 (± 30.3)
S_2: In situ metal-contaminated grassland soil	17.9 (± 0.10)	2175 (± 48.6)	1167 (± 11.5)
S_3: In situ metal-contaminated floodplain soil	16.6 (± 0.94)	5815 (± 378.9)	2949 (± 205.7)

[a]Aqua regia extraction; values represent mean (± SE) of 4 replicates

in vitro breeding with improved metal-phytoextraction and metal tolerance (Herzig et al. 2014; Nehnevajova et al. 2009a). Sunflower seedlings were prepared in May–June 2011, and 1-month-old seedlings (2 seedlings pot^{-1}) were transplanted into pots on July 25–26, 2011. Recommended rate of major-nutrients (N, P, K, Ca, and Mg) was added into soils. Nutrients were added into metal-spiked soils by compensating nitrate-nitrogen supply through spiking of nitrate salts as in case of Cd and Pb treatments. N, P, and K solution was prepared from analytical grade chemical, respectively, NH_4NO_3, K_2HPO_4, and KCl. Plants were irrigated daily with 500 ml deionized water.

Spectral Reflectance Measurement of Leaves

A total of four spectral measurements were done on dissected leaves from each pot in a laboratory. ASD FieldSpec portable spectroradiometer (350–2500 nm at resolution of 1 nm; ASD, Inc., Boulder, CO) was used to collect reflectance spectra using a plant probe leaf-clip assembly fitted with an internal halogen light. The reflectance spectra were measured by holding sunflower leaf into leaf clip holder. Leaf-clip assembly has got two-sided rotating head: a black panel face for reflectance and a white for transmittance measurement. Reflectance spectra were calibrated against a white Spectralon panel face. The use of the leaf clip and contact probe reduces interferences, such as atmospheric disturbances, and unstable light. The leaf clip was repositioned on the same leaf/leaves between each scan to 3–5 different locations, to minimize measurement inaccuracy and to acquire the natural variations in metal-induced stress.

Individual spectral measurement was averaged by treatment to reduce variation, and spectra were corrected for ASD jump (drift correction; additive) using AS-toolbox package (Dorigo et al. 2006) add-in installed in ENVI + IDL version 4.3. First derivative (FD) calculation was done on corrected spectra with 5-point moving average to intensify spectral features. As studied in our previous study, several vegetation indices (VIs) relevant to the metal-induced plant stress, particularly in chlorophyll and water absorption regions, were computed [viz., chlorophyll indices NDVI, LCI, SR705, REIP, and water stress indices NDWI, NDWI_MIR, MSI, LWVI2; Rathod et al. (2015)]. Continuum removal (CR) was applied to corrected spectra which normalizes the reflectance spectra by applying convex hull and amplifies the individual absorption feature (Clark and Roush 1984). Difference in band depths (BDs) between control and metal-treatment was statistically compared for selected absorption region and at specific wavelength (around 495, 680, 970, 1165, 1435, 1780, and 1925 nm) as reported in our previous work (Rathod et al. 2015).

Chemical and Statistical Analysis

At each spectral measurement, the sampled leaves were dried at 80 °C for 24 h and milled. For analyzing total metal content, 250 mg of milled sample was digested with 5 mL concentrated HNO_3 in Teflon tubes in pressurized microwave accelerated reaction system (CEM Mars5 microwave digestion system; Matthews, USA) for 30–40 min. The digested substrate was then diluted with 10 mL deionized water and analyzed for total Cd, Pb, and As using inductively coupled plasma-atomic emission spectrometry (ICPMS X-series instrument, Thermo Fisher Scientific GmbH, Bremen, Germany). Standard reference soil and plant samples (GBW7604, poplar leaves, office of CRM's, China) were also digested for recovery test. Precision for all standards was better than 95%. All chemicals used in chemical analysis were of analytical grade.

Statistical analyses of spectral and chemical data were performed in MS Excel spreadsheets 2007 with XLSTAT 2009.1.02 add-ins and reported at $\alpha = 0.05$ significance level. Mean and standard error (± SE) were computed for all data. Data were statistically tested for significant effects through analysis of variance, and post hoc Tukey HSD test was done to compare the treatment mean. Correlation coefficients (Pearson's '*r*') were computed between spectral variables (i.e., corrected spectra, VIs, BDs of CR spectra) and leaf-metal content for each treatment. The relationship between leaf-metal concentration and spectral features (i.e., correlated spectral wavelength regions, VIs and BDs values) was modeled using regression analysis, leave-one-out cross-validation techniques (PLSR, partial least square regression and MLR, multiple linear regression; in Unscrambler 9.7, CAMO ASA, Norway). Values of coefficient of determination (R^2) between measured and predicted value and root-mean-square error (RMSE) were used to examine the relationship found.

Results and Discussion

Leaf Spectral Reflectance

The leaf reflectance measured at 30, 45, 60, and 90 days of sunflower growth and showed a similar pattern over the growth for most treatments. S_1-Mix and S_3 soils, however, showed spectral variations between spectral measurements at 30 and 45 days (Fig. 1a, b), which was also visible by eye. In response to Cd-spiking into S_1-soil, slight spectral changes in sunflower leaves were observed compared to control spectra (Fig. 2a, b). Leaf reflectance spectra from S_1-Cd_2 spiked pot varied from control plant spectra especially in chlorophyll absorption regions (~ 490–675 nm), as can be seen in the first derivatives spectra (Fig. 2c, d), and in the water absorption regions at around 950, 1150, 1400, and 1900 nm (Fig. 2c, d). Cadmium is known to interfere with uptake of other essential nutrients [Prasad (2004); we also found decreased leaf-Fe and -P concentration for Cd-treated plant compared to control; data not shown] to inhibit chlorophyll synthesis and to alter water balance in tissues (Maria et al. 2013). These stress-induced changes in chlorophyll and water content altogether provide a most generic spectral response in VNIR and water absorption bands (Kancheva and Borisova 2010; Peñuelas and Filella 1998). Slight spectral changes in visible and at the red-edge wavelengths were observed from S_1-Pb treated sunflower compared to control spectra (Fig. 2a–d).

The changes in visible wavelengths were noticeable and showed a larger increase in reflectance for As-treated plant compared to rest of the treatments. An increased reflectance in visible regions and decreased reflectance in NIR

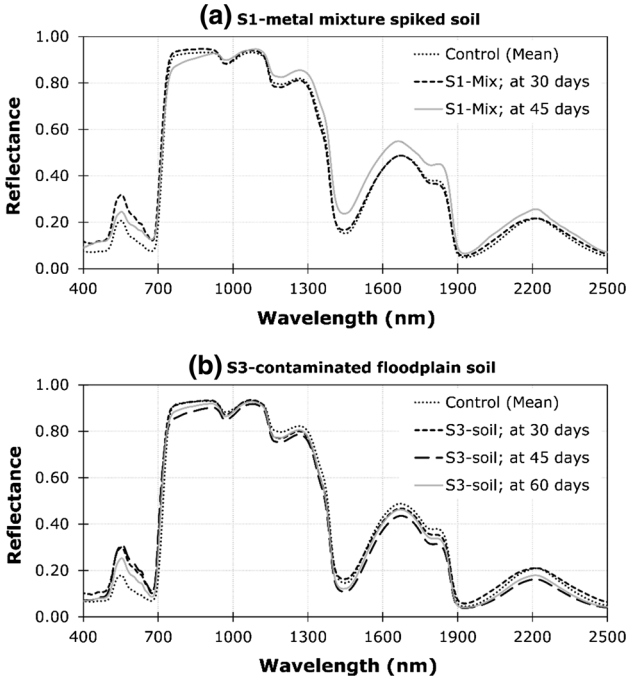

Fig. 1 Reflectance spectra of **a** S_1-Mix and **b** S_3-contaminated floodplain soil treatments at different spectral measurement intervals

regions were substantial in case of S_1-As_2 treatment at 30 days of plant growth (Fig. 2a). A clear difference can be seen in the first derivatives spectra at visible wavelengths (Fig. 2c), wherein red-edge shift to the shorter wavelength was clearly visible, indicating severe As-stress at 900 mg kg^{-1} to the plant. Metal-induced plant stresses result in leaf chlorophyll loss that usually cause reduction in the absorption band in red, and a red-edge shift to shorter wavelengths (Horler et al. 1983) is consistent with present result. Similar result has been reported in other studies of sunflower exposed to metal-contamination (de Gandy 2010).

For metal-mixture spiking (S_1-Mix) and in situ metal-contaminated soils (S_2 and S_3), substantial changes in the leaf reflectance were found mainly in the red-edge, NIR and water absorption regions of spectrum at 45 days of plant growth, especially with sunflower grown in S_3-soil (Fig. 2e, f), which was severely contaminated with Pb and As-metals (Table 1). Similar spectral changes also found with S_1-Mix treatment, while moderate spectral changes were noticed for S_2-soil compared to the control plant spectra. These spectral changes with in situ metal-contaminated soils illustrate metals' additive toxic effects upon their higher accumulation into plant parts (data not presented). At higher concentration, arsenic interferes with plant metabolic processes and can inhibit growth, often leading to the plant death (Garg and Singla 2011).

Pearson's correlation coefficients between reflectance spectra and leaf-metal concentration were computed for all

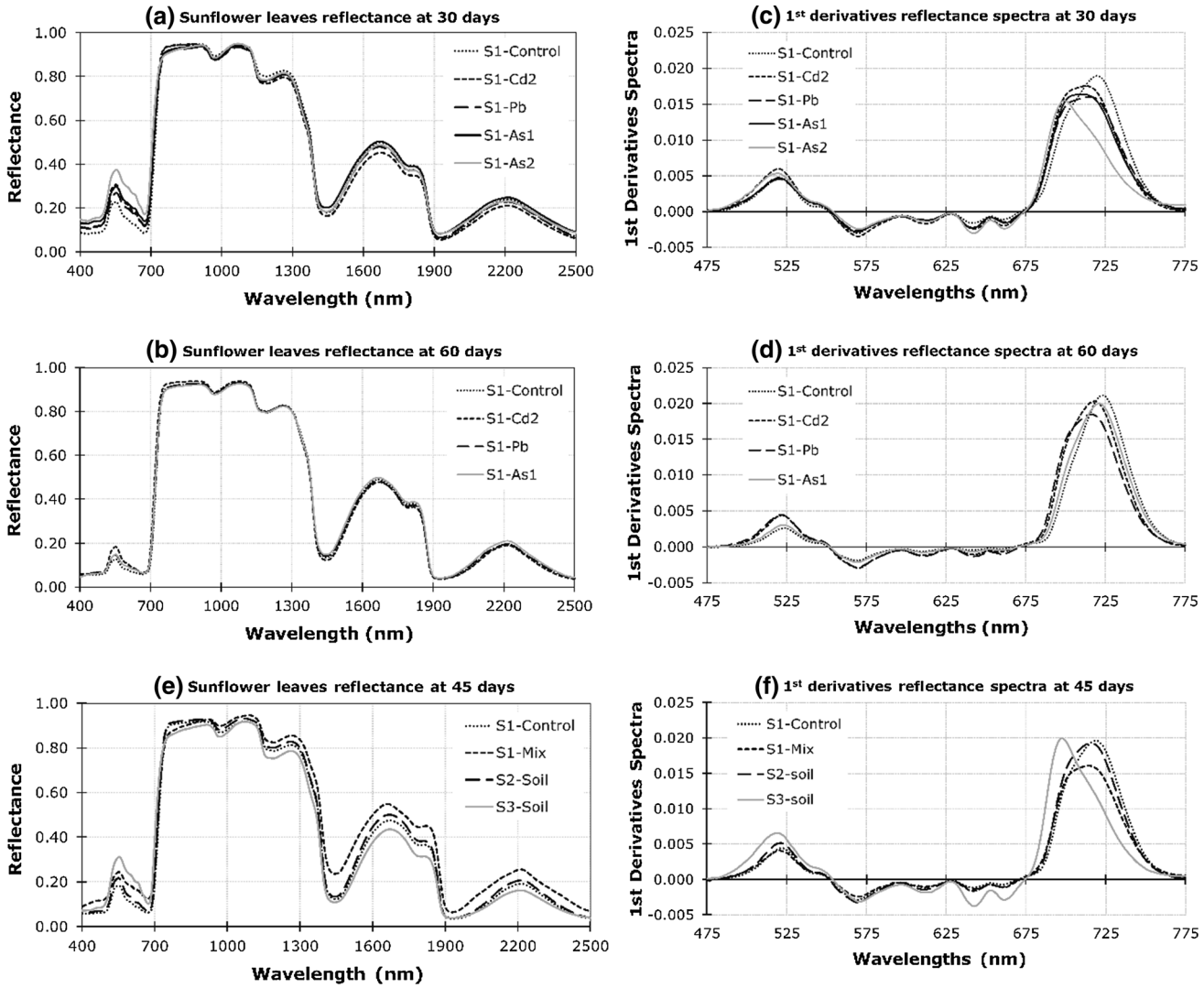

Fig. 2 Reflectance spectra (**a**, **b**, **e**) and their first derivatives reflectance spectra (**c**, **d**, **f**) of leaves of sunflower grown in metal-spiked soils at 30 and 60 days, and in in situ metal-contaminated soils at 45 days of plant growth

observations within the respective treatment set. The correlograms of leaf-metal content and reflectance across the entire spectrum show the highest degree of overall correlation for visible and water absorption regions of the spectrum Fig. 3a–c). Generally, on 30 and 45 days, for S_1-Cd treatment set, ~ 470–750 nm (r = 0.58 to 0.76), and for S_1-Pb treatment set, ~ 415–690 nm (r = 0.72 to 0.94) wavelengths showed significant ($p < 0.05$) positive correlation, respectively, with leaf-Cd and -Pb metal concentration (Fig. 3a–c). While, NIR and water absorption wavelengths showed significant negative correlations, i.e., on 30 days, wavelengths 950–1006 nm (r = − 0.58 to − 0.65), 1127–1908 (r = − 0.58 to − 0.73) with leaf-Cd; 744–955 nm (r = − 0.71 to − 0.94) with leaf-Pb. On 45 days, 1389–1438 and 1866–1893 nm wavelengths yield negative correlation (r = − 0.58 to − 0.65) with leaf-Cd. In case of metal-mixture (S_1-Mix)-spiked and in situ contaminated soils (S_2 and S_3 soils) treatment sets on 30 days, reflectance in visible regions showed significant positive correlation with leaf-metal concentrations (Fig. 3c), i.e., ~ 400–700 (r = 0.50 to 0.88) for leaf-Cd, ~ 451–690 (r = 0.50 to 0.55) for leaf-Pb, ~ 450–690 (r = 0.50 to 0.69) for leaf-As concentration. The observed positive correlation for visible wavelengths at the initial growth periods might be associated with reduction in chlorophyll as a manifestation of metallic-ion toxicity. Such VNIR spectral variations in sunflower leaves due to mineral deficiencies and metal-toxicity have been reported in other studies (Mariotti et al. 1996; Peñuelas et al. 1994) are in agreement with our results. With respect to spiked metal concentration and background levels in soils, these elements are known phytotoxins (Gallego et al. 1996; Imran et al. 2015; Kabata-Pendias and Pendias 2001; Raba

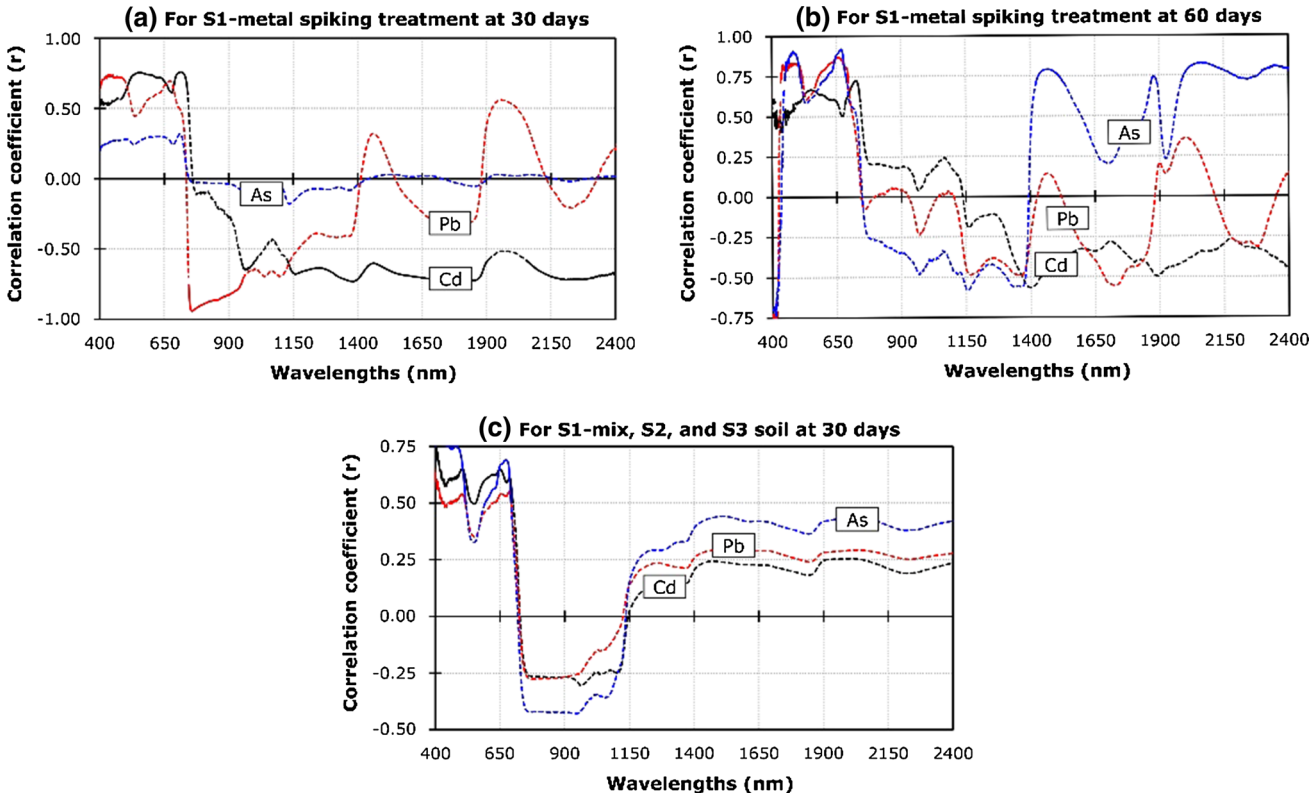

Fig. 3 Pearson's correlation (*r*) of reflectance spectra against leaf-metal concentration for (**a**, **b**) S1-Cd, -Pb, and -As-spiking treatments at 30 and 60 days and **c** for S_1-metal-mixture, S_2, and S_3 treatments at 30 days. Solid line represents significant correlation between wavelength and metal concentration at $\alpha = 0.05$ level, and dotted line represents nonsignificant correlations

et al. 2005) that may have caused damage to chlorophyll and leaf structure of the sunflower plant.

Vegetation Indices and Continuum Removed Spectra

Generally, the Cd-spiking to S_1-soil showed nonsignificant changes in the calculated indices compared to indices obtained from untreated plant spectra (Fig. 4). Treatment S_1-Pb_1 showed significant decrease in SR705 index compared to control treatment at 30 days, i.e., 2.853 against 4.064. However, S_1-Pb_1 shows no significant difference in other calculated indices from control plants. The REIPs (Savitzky–Golay Filter first-order derivative and smoothing technique) also decreased (i.e., shifted toward blue wavelengths) for Cd- and Pb-spiking, but was found nonsignificant with respect to control REIPs.

As seen in Fig. 4, the arsenic and metal-mixture spiking to S_1-soils can statistically be distinguished from untreated plants. On 30 days of sowing, the least values of NDVI, LCI, and SR705 obtained with As-spiking at 900 mg kg^{-1} to S_1-soils (0.685, 0.268, and 2.110, respectively) followed by multi-metal-spiking to S_1-soils (0.726, 0.310, and 2.565, respectively) are significantly differed from untreated plant (0.832, 0.440, and 4.064, respectively). The REIPs are also significantly different from untreated plants for S_1-As_2 and S_1-Mix treatments, a *blue shift* by 20 and 13 nm, respectively, observed. However, these indices for As-spiking at 100 mg kg^{-1} to S_1-soils significantly on par with indices from untreated plant, indicated that spiked level of 100 mg As kg^{-1} is within the tolerance limit for mutant sunflower plant and did not cause plant stress. Similarly, plants grown in in situ contaminated floodplains soils (S_3-soil) can be differentiated using NDVI, LCI and SR705 indices, since these values are significantly lower than those of control treatment on 30, 45, and 60 days (Fig. 4). Moreover, REIPs for S_3-soil treatment show significant *blue shift* by 14, 21, and 18 nm comparative to the control REIP on 30, 45, and 60 days, respectively. A decrease in the values of chlorophyll indices and *blue shift* of REIPs with S_1-As_2, S_1-Mix and S_3-soil could be due to indirect effects of metal-accumulation in plant parts, specifically into roots (data not presented), on photosynthetic activities and chlorophyll synthesis, which altogether lead to changed plant spectral reflectance. Present results are in agreement with several studies that have demonstrated the *blue shift* of REIPs and effectiveness of different chlorophyll indices for the delineation of metal-induced stress-

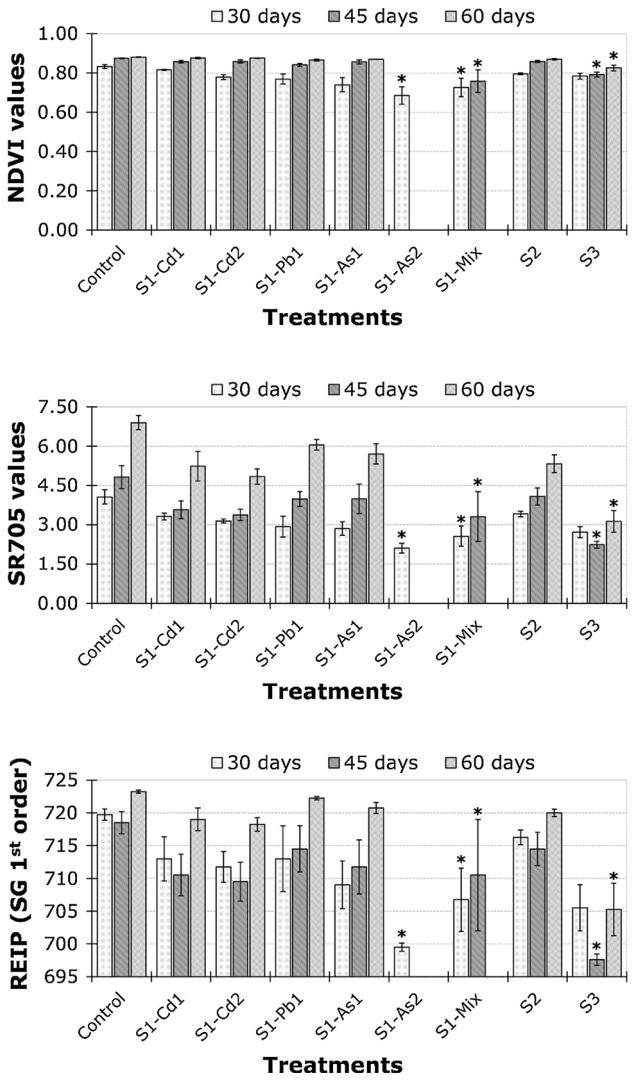

Fig. 4 Changes in chlorophyll vegetation indices (NDVI and SR705) and REIP (SG 1st order) for different metal-contamination treatments. Error bars are values of ± SEm of 3–4 replicates. The columns with asterisk (*) are significantly differed from control treatment at $\alpha = 0.05$ according to post hoc Tukey HSD test

related variations (Li et al. 2015; Milton et al. 1989; Slonecker et al. 2009; Sridhar et al. 2007a, 2014).

Water indices (NDWI, NDWI_MIR, MSI, and LWVI2) are found to be lower for metal-spiking treatments (except S_1-As_2; wherein plants died at 30 days) as well as for S_2- and S_3-soils than the control treatment, but the differences found statistically nonsignificant. This might be owed to either an efficient metal tolerance mechanism of M_5 sunflower mutants toward stress, particularly drought-stress or a well-development root growth, that can lead to improved access to water, minerals, and toxic metal as well (Nehnevajova et al. 2009b; Schwitzguébel et al. 2008). Hence, least spectral variations observed in domains of water absorption regions for moderately metal-spiked or contaminated soils.

Continuum removal (CR; in ENVI-IDL version 4.3) technique was applied and absorption features around 495, 680, 970, 1165, 1435, 1780, and 1925 nm were recognized by visual analyses and by considering typical absorption features noted in the literature (Boyd et al. 2006; Curran 1989). Band depths (BDs = 1−CR reflectance spectra) at selected bands in each absorption features were calculated. The absorption features in visible region (at 495 and 680 nm) can be associated to chlorophyll, 970 nm to the water, at 1165 nm to the biochemical of lignin, 1435 nm to the water or nitrogen, 1780 nm to cellulose or lignin, and 1925 nm to the cellulose or water. The CR spectra and BDs difference between control and metal-contamination treatments at 30 and 45 days are shown, respectively, in Fig. 5a–d. Generally, spectra of control plants had the deepest BDs in considered absorption regions. The BDs for plant grown in Cd- and Pb-spiked soils were same as observed for control plants. The lowest BDs and greatest positive BDs difference relative to control (i.e., shallower BDs than control) noted for S_1-As_2, S_1-Mix, and S_3 treatments, most prominent in red-edge (550–750 nm) and water absorption (1371–1675, 1850–2250 nm) regions. This demonstrates phytotoxic effects of metals on sunflower plant and significant changes in leaf spectral reflectance. Absorption features in red-edge region are strongly governed by foliar pigment concentration which characteristically decreases due to abiotic stress. While, absorption features within 1371–1675 and 1850–2250 nm wavelengths related to the biochemical of water, nitrogen, lignin, and cellulose (Boyd et al. 2006; Curran 1989; Curran et al. 2001; Huber et al. 2008), and there might be selective depletion of these biochemicals due to phytoaccumulation of toxic metals into plant parts, and it can be revealed through spectral changes (Götze et al. 2010).

Pearson's correlation results reported in Table 2 indicate a significant effect of metal-spiking to S_1-soil on sunflower leaf spectral properties related with chlorophyll absorption, while no other treatments were found to be statistically significant. Leaf-Cd and -As concentration are strongly correlated with LCI ($r = -0.707$; $p = 0.0001$ and $r = -0.544$; $p = 0.013$), while lead-Pb correlated with PRI ($r = -0.710$; $p = 0.002$). Leaf-As also showed an inverse relationship with band depth at 680 nm ($r = 0.465$; $p = 0.039$), that is associated with chlorophyll absorption (Buschmann and Nagel 1993; Curran et al. 1992; Gitelson and Merzlyak 1996).

Regression Analysis

Partial least square regression (PLSR) analysis was performed to relate leaf-metal concentration to the leaf

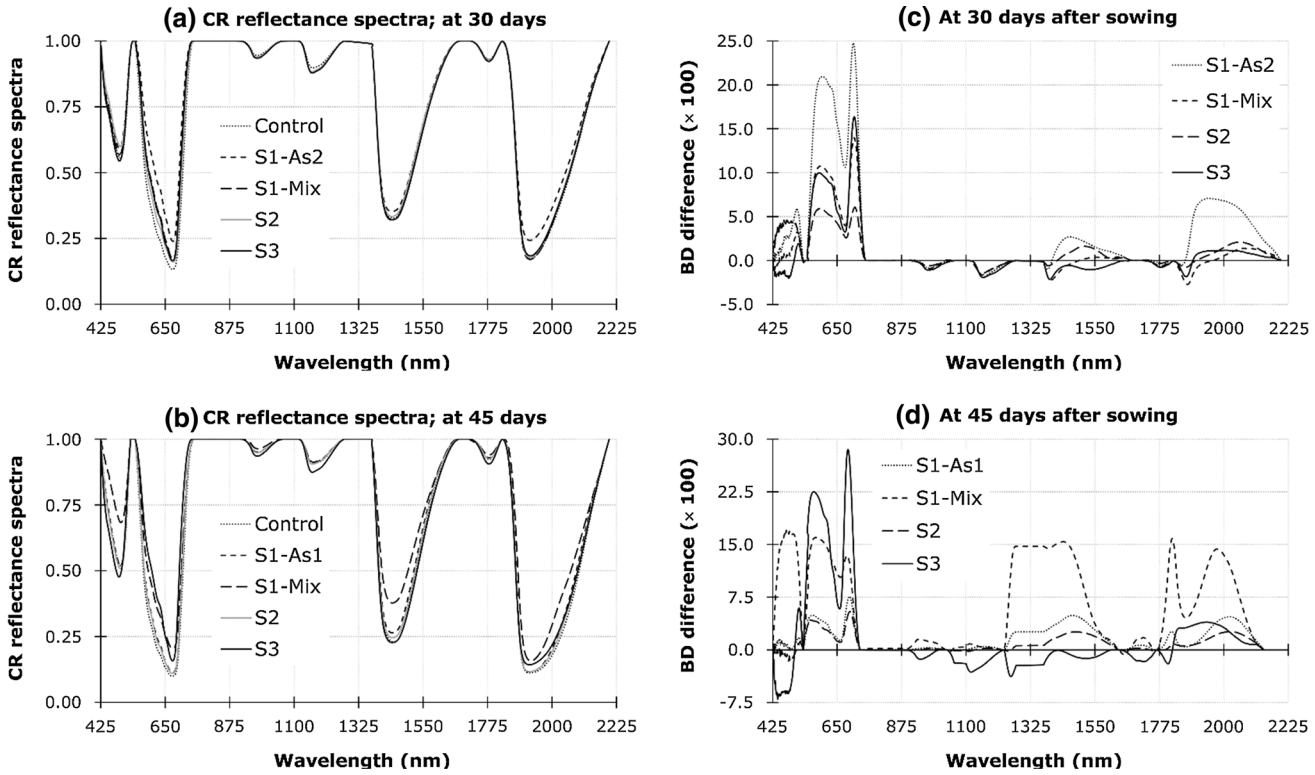

Fig. 5 Continuum removed spectra of control and metal-contamination treatments at **a** 30 and **b** 45 days of plant growth. Band depth difference between control and metal-contamination treatments at **c** 30 and **d** 45 days. Positive difference indicates greater absorption (or deeper band depths) in control than metal-contaminated soils. Treatments S_1-As_2 and S_3 cause the largest differences

Table 2 Correlation coefficient (r) of leaf-metal concentration to vegetation indices and band depths at selected wavelengths within the CR absorption regions

VIs and BDs	Leaf-Cd concentration[a]		Leaf-Pb concentration[a]		Leaf-As concentration[a]	
	Pearson 'r'	p values	Pearson 'r'	p values	Pearson 'r'	p values
NDVI	− 0.281	0.183	**− 0.506**	**0.046**	− 0.433	0.056
LCI	**− 0.707**	**0.0001**	− 0.418	0.107	**− 0.544**	**0.013**
SR705	**− 0.630**	**0.001**	− 0.465	0.069	− 0.368	0.110
PRI	**− 0.445**	**0.029**	**− 0.710**	**0.002**	− 0.366	0.112
REIP	**− 0.626**	**0.001**	− 0.345	0.190	− 0.422	0.064
NDWI	**0.447**	**0.029**	− 0.122	0.653	0.114	0.634
NDWI_MIR	**0.414**	**0.044**	− 0.163	0.546	− 0.055	0.819
MSI	**− 0.645**	**0.001**	0.284	0.286	− 0.049	0.837
BD_495	**0.452**	**0.027**	**− 0.544**	**0.003**	− 0.375	0.104
BD_680	− 0.248	0.242	− 0.328	0.215	**− 0.465**	**0.039**
BD_970	**0.431**	**0.035**	0.025	0.927	0.254	0.279
BD_1165	**0.500**	**0.013**	0.167	0.538	0.214	0.366
BD_1780	**0.497**	**0.014**	− 0.236	0.378	− 0.339	0.144

[a]correlation coefficients were calculated for pooled datasets of control and S_1-metal-spiking treatments on 30 and 45 days, i.e., for S_1-Cd spike, n = 24; S_1-Pb spike, n = 16, and S_1-As spike, n = 20. No significant correlation found for S_1-Mix, S_2, and S_3 treatment datasets, hence data not given. Values in bold are different from 0 with a significance level α = 0.05

reflectance spectra (raw and first derivatives). The PLS regression reduces the large number of measured collinear spectral variables to a few non-correlated latent variables or factors (Abdi 2003). The factors represent the relevant information in the measured leaf spectral reflectance and are used to predict the dependent variable, herein leaf-

metal concentration. We also tested MLR built upon the vegetation indices and BDs values at selected wavelengths within the absorption features. Due to small sample size, each treatment dataset collected on 30 and 45 days was combined to improve the statistical significance of the models. Table 3 and Fig. 6 depict the cross-validated calibration results of R^2 and RMSE using PLSR and MLR analysis. The final models, which were selected by high R^2 and low root-mean-square error (RMSE) values of cross-validated analysis in each dataset, included different spectral wavelengths data.

The PLSR using raw reflectance spectra found to be inferior to models based on Savitzky–Golay filter first-order derivative spectra. A combination of vegetation indices, as well as BDs within selected absorption features also proved to be good predictors of leaf-metal variability. The important wavelengths with significant regression coefficient were selected for PLSR modeling according to Martens' uncertainty test (Westad and Marten 2000) performed with cross-validation, and those wavelengths are mostly centered around chlorophyll absorption, red-edge, near infrared, and water absorption regions. For the leaf-Cd estimation, the best PLSR model based on significant FD spectral wavelengths (i.e., 607–10, 1067, 1332–33, 1338–45 nm) obtained in the combined datasets of control, S_1-Cd treatments (n = 19) that yielded R^2, 0.913, and RMSE, 6.251 for validation model (Table 3). Good predictive model for leaf-Cd estimation (R^2, 0.913, and RMSE, 6.251) similarly also obtained for control, S_1-Mix, S_2, and S_3 treatment dataset (n = 25) using significant FD spectra. Relatively, inferior predictions of leaf-Cd were achieved with MLR models based on all VIs and BDs (R^2, 0.600, and RMSE, 13.924) for control and S_1-Cd treatments dataset. Likely, the PLSR and MLR models, respectively, based on significant FD spectral wavelengths (within the 400–2200 nm) and all VIs, BDs showed robust assessment of leaf-Pb (R^2, 0.946 and 0.989, and RMSE, 11.295 and 4.579; validation model) for control and S_1-Pb treatment dataset. The models for leaf-Pb estimation found inferior for control, S_1-Mix, S_2, and S_3 treatment dataset. For estimation of leaf-As concentration, only visible spectral regions (400–800 nm) were found to be particularly suitable, and the cross-validation performance further improved using most significant wavelengths within visible region (Table 3). The best fit model of leaf-As estimation was obtained with R^2, 0.962 and RMSE, 8.027 for control, S_1-As treatment dataset (n = 18). Similarly, for dataset of control, S_1-Mix, S_2, and S_3 treatments (n = 28), the best fit

Table 3 Best-fit PLSR and MLR models for estimation of sunflower leaf-metal concentration

Regression models		R^2 cal.	R^2 val.	RMSE cal.	RMSE val.
For the prediction of Leaf-Cd concentration					
1.	PLSR_FD full spectra (400–2200 nm); for control, S_1-Cd dataset, n = 19; PC#4	0.848	0.660	7.816	12.336
2.	PLSR_FD significant WL[a]; for control, S_1-Cd dataset, n = 19, PC#3	0.934	0.913	5.125	6.251
3.	PLSR_FD significant WL[b]; for control, S_1-Mix, S_2, S_3 dataset, n = 25, PC#3	0.906	0.856	4.702	6.073
4.	MLR with selected VIs and BDs[c]; for control, S_1-Cd dataset, n = 22	0.899	0.600	6.977	13.924
For the prediction of Leaf-Pb concentration					
5.	PLSR_ FD significant WL[d]; for control, S_1-Pb dataset, n = 15; PC#5	0.977	0.946	6.866	11.295
6.	MLR with all VIs and BDs at 495, 970, 1780 nm; for control, S_1-Pd dataset, n = 15	0.999	0.989	0.379	4.579
For the prediction of Leaf-As concentration					
7.	PLSR_FD spectra (400–800 nm); for control, S_1-As dataset, n = 20; PC#7	0.981	0.641	5.123	24.042
8.	PLSR_FD significant WL[e] within 400–800 nm; for control, S_1-As dataset, n = 18; PC#4	0.979	0.962	5.585	8.027
9.	PLSR_FD significant WL[f] within 400–800 nm; for control, S_1-Mix, S_2, S_3 dataset, n = 28; PC#7	0.995	0.825	17.115	35.062
10.	MLR with all VIs; for control, S_1-As dataset, n = 17	0.977	0.890	7.108	15.573

Model is expressed in terms of coefficients of determination (R^2) and root-mean-square error (RMSE) of calibration, cal and cross-validation, val models

[a]Significant FD wavelengths are: 607–10, 1067, 1332–33, 1338–45 nm

[b]Significant FD wavelengths are: 470, 476–77, 780, 979–81, 1078, 1172–76, 1182–83, 1193–96, 1202–04, 1372, 1438–39, 1790–93 nm

[c]Selected VIs and BDs are: NDVI, LCI, SR705, PRI, NDWI, NDWI_MIR, BD_495, and BD_1165

[d]Most significant FD wavelengths are within the chlorophyll absorption, red-edge, near infrared, and water absorption regions

[e]Singificant FD wavelengths are: 411, 426, 432, 535–40, 545, 677–79 nm

[f]Significant FD wavelengths are: 410–11, 417–20, 421, 425–26, 434, 465–66, 473–74, 476–77, 481, 488–92, 499, 587–88, 695–695 nm

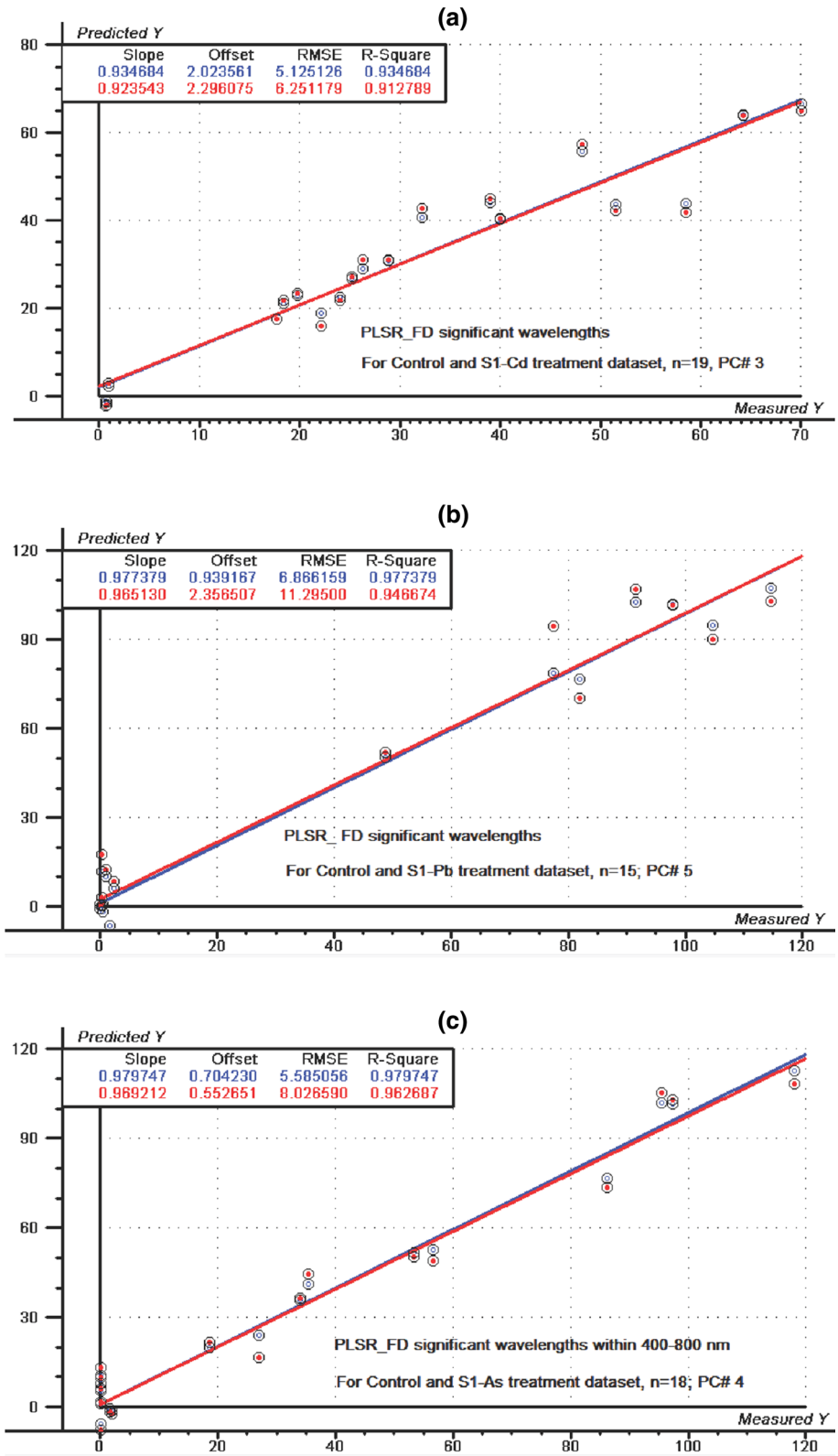

Fig. 6 Scatter plot of measured versus predicted leaf-Cd (**a**), Leaf-Pb (**b**), leaf-As (**c**) concentration using PLSR calibration models. Blue and red lines, respectively, represent the results of calibration and validation models. See footnote at Table 3 for detail of significant wavelengths

model of leaf-As estimation was obtained with R^2, 0.825, and RMSE, 35.062. The MLR calibration model based on all calculated VIs also yielded good prediction results (R^2, 0.890, and RMSE, 15.573) of leaf-As for control, S_1-As treatment dataset (n = 18).

For all PLSR analysis, the FD wavelengths with significant regression coefficient (i.e., relationship between predictor wavelengths and response variable leaf-metal concentration; important wavelengths are given at footnote at Table 3) used in the models are associated with chlorophyll absorption, red-edge position, and water absorption regions of spectrum. This finding is coherent with observed vegetation spectral pattern due to soil metal-contamination, and it has been also studied by Bandaru et al. (2010); Hong et al. (2010); Slonecker et al. (2009) for different test crops and soil metal-contamination.

Conclusion

Leaf reflectance obtained from sunflower grown in metal-contaminated soils was varied in chlorophyll absorption and NIR domains of spectrum, and it shows the highest degree of overall correlation with leaf-metal concentration. For both metal-spiked and in situ contaminated soils, positive correlations with visible spectrum, while negative correlations with NIR and water absorption bands, were found. Sunflower grown in metal-spiked soil (i.e., S_1-As_2 and S_1-Mix metals) and in in situ metal-contaminated soils might possibly be examined at early growth stages through chlorophyll vegetation indices LCI, SR705, and REIP, as of these indices were found significantly different from the control values. Shifting of red-edge inflection points by $\sim$ 20 nm toward blue wavelength is evident of metal-induced plant stress. Similarly, first derivatives of reflectance, continuum removed absorption features, and band depth values were found to be the promising spectral features in monitoring plant health during phytoremediation process. Regardless of the kind and number of stressors, the changes in spectral properties is mainly linked to an alteration in chlorophyll concentration, water balance, and/or leaf morphology. Thus, if the specific stressor is known (metal-induced stress, for example, in present sunflower study), the measurement of spectral properties is useful for monitoring early metal-toxicity in plant, but it could be challenging to distinguish them among individual metal-induced plant stress. Multivariate regression approaches confirmed that obtained PLSR and MRL models, respectively, based on first derivative spectral reflectance and spectral feature likes VIs and BDs could provide good estimation of the leaf-metal variation. The results demonstrate that it is feasible to use plant spectral reflectance for monitoring of physiological stress caused by metal contaminants during the process of phytoextraction. As the spectral variations have been observed at the leaf level under stable illuminated source in the laboratory, they have to be further verified at the canopy level and on the metal-contaminated sites for extending the applications of hyperspectral remote sensing.

Acknowledgements The authors would like to acknowledge the European Commission Higher Education Program for Granting Erasmus Mundus External Cooperation Window Scholarship to support this research. Special thanks to faculties at Department of Earth System Analysis, ITC, University of Twente; at Institute of General Ecology and Conservation, Tharandt, TU Dresden; and at Saxon State Office for Environment, Agriculture and Geology, Freiberg, for their invaluable technical assistance. The authors are specially thankful to Dr. Rolf Herzig, Phytotech Foundation, Bern, Switzerland, for providing with the seeds of sunflower M5 mutant lines – M5/R4-R6/15-35-190-04-M5.

References

Abdi, H. (2003). Partial least square regression (PLS regression). In Lewis-Beck, T. F. Liao, & A. Bryman (Eds.), *The SAGE encyclopedia of social science research methods* (Vol. 1, pp. 792–795). Thousand Oaks: Sage.

Adesodun, J., Atayese, M., Agbaje, T. A., Osadiaye, B., Mafe, O. F., & Soretire, A. (2010). Phytoremediation potentials of sunflowers (Tithonia diversifolia and Helianthus annuus) for metals in soils contaminated with zinc and lead nitrates. *Water, Air, and Soil Pollution, 207*(1–4), 195–201. https://doi.org/10.1007/s11270-009-0128-3.

Bandaru, V., Hansen, D. J., Codling, E. E., Daughtry, C. S., White-Hansen, S., & Green, C. E. (2010). Quantifying arsenic-induced morphological changes in spinach leaves: Implications for remote sensing. *International Journal of Remote Sensing, 31*(15), 4163–4177. https://doi.org/10.1080/01431161.2010.498453.

Blackburn, G. (2007). Hyperspectral remote sensing of plant pigments. *Journal of Experimental Botany, 58*(4), 855–867. https://doi.org/10.1093/jxb/erl123.

Boyd, D., Entwistle, J., Flowers, A., Armitage, R., & Goldsmith, P. (2006). Remote sensing the radionuclide contaminated Belarusian landscape: A potential for imaging spectrometry? *International Journal of Remote Sensing, 27*(10), 1865–1874. https://doi.org/10.1080/01431160500328355.

Buschmann, C., & Nagel, E. (1993). In vivo spectroscopy and internal optics of leaves as basis for remote sensing of vegetation. *International Journal of Remote Sensing, 14*(4), 711–722. https://doi.org/10.1080/01431169308904370.

Clark, R. N., & Roush, T. L. (1984). Reflectance spectroscopy: Quantitative analysis techniques for remote sensing applications. *Journal of Geophysical Research: Solid Earth, 89*(B7), 6329–6340. https://doi.org/10.1029/JB089iB07p06329.

Cundy, A., Bardos, R. P., Puschenreiter, M., Mench, M., Bert, V., Friesl-Hanl, W., et al. (2016). Brownfields to green fields: Realising wider benefits from practical contaminant phytomanagement strategies. *Journal of Environmental Management, 184*(1), 67–77. https://doi.org/10.1016/j.jenvman.2016.03.028.

Cundy, A., Bardos, P., Puschenreiter, M., Witters, N., Mench, M., Bert, V., et al. (2015). Developing effective decision support for the application of "gentle" remediation options: The GREENLAND project. *Remediation Journal, 25*(3), 101–114. https://doi.org/10.1002/rem.21435.

Curran, P. J. (1989). Remote sensing of foliar chemistry. *Remote Sensing of Environment, 30*(3), 271–278. https://doi.org/10.1016/0034-4257(89)90069-2.

Curran, P. J., Dungan, J. L., Macler, B. A., Plummer, S. E., & Peterson, D. L. (1992). Reflectance spectroscopy of fresh whole leaves for the estimation of chemical concentration. *Remote Sensing of Environment, 39*(2), 153–166. https://doi.org/10.1016/0034-4257(92)90133-5.

Curran, P. J., Dungan, J. L., & Peterson, D. L. (2001). Estimating the foliar biochemical concentration of leaves with reflectance spectrometry: Testing the Kokaly and Clark methodologies. *Remote Sensing of Environment, 76*(3), 349–359. https://doi.org/10.1016/S0034-4257(01)00182-1.

Cuypers, A., Smeets, K., & Vangronsveld, J. (2009). Heavy metal stress in plants. In H. Hirt (Ed.), *Plant Stress Biology: From Genomics to Systems Biology* (pp. 161–178). KGaA, Weinheim: Wiley-VCH. https://doi.org/10.1002/9783527628964.ch8.

de Gandy, Y. P. P. (2010). *Spectral reflectance as an indicator of foliar concentrations of arsenic in common sunflower (Helianthus Annuus).* M.S. dissertation No. 1488735. Department of Chemistry, University of Texas-Pan American.

Dorigo, W., Bachmann, M., & Heldens, W. (2006). *AS toolbox and processing of field spectra: Use's manual, Version 1.13*. Wessling: German Aerospace Center (DLR), German Remote Sensing Data Center, Institute for Environment and Geoinformation Team Imaging Spectroscopy.

Font, R., del Río-Celestino, M., & de Haro-Bailón, A. (2007). Near-infrared reflectance spectroscopy: Methodology and potential for predicting trace elements in plants. In N. Willey (Ed.), *Phytoremediation, methods and reviews* (Vol. 23). Totowa, NJ: Humana Press Inc.

Gallego, S. M., Benavides, M. P., & Tomaro, M. L. (1996). Effect of heavy metal ion excess on sunflower leaves: Evidence for involvement of oxidative stress. *Plant Science, 121,* 151–159. https://doi.org/10.1016/S0168-9452(96)04528-1.

Garg, N., & Singla, P. (2011). Arsenic toxicity in crop plants: Physiological effects and tolerance mechanisms. *Environmental Chemistry Letters, 9*(3), 303–321. https://doi.org/10.1007/s10311-011-0313-7.

Gitelson, A. A., & Merzlyak, M. N. (1996). Signature analysis of leaf reflectance spectra: Algorithm development for remote sensing of chlorophyll. *Journal of Plant Physiology, 148*(3), 494–500. https://doi.org/10.1016/S0176-1617(96)80284-7.

Götze, C., Jung, A., Merbach, I., Wennrich, R., & Gläßer, C. (2010). Spectrometric analyses in comparison to the physiological condition of heavy metal stressed floodplain vegetation in a standardised experiment. *Open Gioscience (Formerly Central European Journal of Geosciences), 2*(2), 132–137. https://doi.org/10.2478/v10085-010-0002-y.

Herzig, R., Nehnevajova, E., Pfistner, C., Schwitzguebel, J.-P., Ricci, A., & Keller, C. (2014). Feasibility of labile Zn phytoextraction using enhanced tobacco and sunflower: Results of five-and one-year field-scale experiments in Switzerland. *International Journal of Phytoremediation, 16,* 735–754. https://doi.org/10.1080/15226514.2013.856846.

Hong, H., Feng-jie, Y., Guang-zhu, Z., & Yin-ming, L. (2010). Spectral features and regression model of mine vegetation in the press of heavy metal. In *Second International Workshop on Education Technology and Computer Science* (pp. 57–59). IEEE. https://doi.org/10.1109/etcs.2010.398.

Horler, D. N. H., Barber, J., & Barringer, A. R. (1980). Effects of heavy metals on the absorbance and reflectance spectra of plants. *International Journal of Remote Sensing, 1,* 121–136. https://doi.org/10.1080/01431168008547550.

Horler, D. N. H., Dockray, M., & Barber, J. (1983). The red edge of plant leaf reflectance. *International Journal of Remote Sensing, 4*(2), 273–288. https://doi.org/10.1080/01431168308948546.

Huber, S., Kneubuhler, M., Psomas, A., Itten, K., & Zimmermann, N. E. (2008). Estimating foliar biochemistry from hyperspectral data in mixed forest canopy. *Forest Ecology and Management, 256,* 491–501. https://doi.org/10.1016/j.foreco.2008.05.011.

Imran, M. A., Sajid, Z. A., & Chaudhary, M. N. (2015). Arsenic (As) toxicity to germination and vegetative growth of sunflower (*Helianthus annuus L.*). *Poland Journal of Environment Studies, 24*(5), 1993–2002. https://doi.org/10.15244/pjoes/39553.

Kabata-Pendias, A., & Pendias, H. (2001). *Trace elements in soils and plants* (3rd ed.). Boca Raton: CRC Press LLC.

Kancheva, R., & Borisova, D. (2010). Spectral data for plant chlorophyll assessment. *Sovremennye problemy distantsionnogo zondirovaniya Zemli iz kosmosa*, *7*(3), 239–245.

Kidd, P., Mench, M., Álvarez-López, V., Bert, V., Dimitriou, I., Friesl-Hanl, W., et al. (2015). Agronomic practices for improving gentle remediation of trace element-contaminated soils. *International Journal of Phytoremediation, 17*(11), 1005–1037. https://doi.org/10.1080/15226514.2014.1003788.

Li, X., Liu, X., Liu, M., Wang, C., & Xia, X. (2015). A hyperspectral index sensitive to subtle changes in the canopy chlorophyll content under arsenic stress. *International Journal of Applied Earth Observation and Geoinformation, 36,* 41–53. https://doi.org/10.1016/j.jag.2014.10.017.

Maria, S. D., Puschenreiter, M., & Rivelli, A. R. (2013). Cadmium accumulation and physiological response of sunflower plants to Cd during the vegetative growing cycle. *Plant Soil Environment, 59*(6), 254–261.

Mariotti, M., Ercoli, L., & Masoni, A. (1996). Spectral properties of iron-deficient corn and sunflower leaves. *Remote Sensing of Environment, 58*(3), 282–288. https://doi.org/10.1016/S0034-4257(96)00070-3.

Mench, M., Lepp, N., Bert, V., Schwitzguébel, J.-P., Gawronski, S. W., Schröder, P., et al. (2010). Successes and limitations of phytotechnologies at field scale: Outcomes, assessment and outlook from COST Action 859. *Journal of Soils and Sediments, 10*(6), 1039–1070. https://doi.org/10.1007/s11368-010-0190-x.

Milton, N. M., Ager, C. M., Eiswerth, B. A., & Power, M. S. (1989). Arsenic-and selenium-induced changes in spectral reflectance and morphology of soybean plants. *Remote Sensing of Environment, 30*(3), 263–269. https://doi.org/10.1016/0034-4257(89)90068-0.

Nehnevajova, E., Herzig, R., Bourigault, C., Bangerter, S., & Schwitzguébel, J.-P. (2009a). Stability of enhanced yield and metal uptake by sunflower mutants for improved phytoremediation. *International Journal of Phytoremediation, 11*(4), 329–346. https://doi.org/10.1080/15226510802565394.

Nehnevajova, E., Herzig, R., Federer, G., Erismann, K.-H., & Schwitzguébel, J.-P. (2005). Screening of sunflower cultivars for metal phytoextraction in a contaminated field prior to mutagenesis. *International Journal of Phytoremediation, 7*(4), 337–349. https://doi.org/10.1080/16226510500327210.

Nehnevajova, E., Herzig, R., Schwitzguébel, J. P., & Schmülling, T. (2009b). Sunflower mutants with improved growth and metal accumulation traits show a potential for soil decontamination. In Q. Y. Shu (Ed.), *Induced plant mutations in the genomics era* (pp. 83–86). Rome: Food and Agriculture Organization of the United Nations.

Noomen, M. F. (2007). *Hyperspectral reflectance of vegetation affected by underground hydrocarbon gas seepage*. Ph.D. Thesis. Faculty of Geoscience and Earth Observation, University of Twente, The Netherlands. https://webapps.itc.utwente.nl/librarywww/papers_2007/phd/noomen.pdf.

Onwubuya, K., Cundy, A., Puschenreiter, M., Kumpiene, J., Bone, B., Greaves, J., et al. (2009). Developing decision support tools for the selection of "gentle" remediation approaches. *Science of the Total Environment, 407*(24), 6132–6142. https://doi.org/10.1016/j.scitotenv.2009.08.017.

Peñuelas, J., & Filella, I. (1998). Visible and near-infrared reflectance techniques for diagnosing plant physiological status. *Trends in Plant Science, 3*(4), 151–156. https://doi.org/10.1016/S1360-1385(98)01213-8.

Peñuelas, J., Gamon, J. A., Fredeen, A. L., Merino, J., & Field, C. B. (1994). Reflectance indices associated with physiological changes in nitrogen- and water-limited sunflower leaves. *Remote Sensing of Environment, 48,* 135–146. https://doi.org/10.1016/0034-4257(94)90136-8.

Pilon-Smits, E. (2005). Phytoremediation. *Annual Review of Plant Biology, 56,* 15–39. https://doi.org/10.1146/annurev.arplant.56.032604.144214.

Prasad, M. N. V. (2004). *Heavy metal stress in plants: From molecules to ecosystems* (2nd ed.). New Delhi: Springer and Jointly published with Narosa Publishing House.

Prasad, M. N. V., & de Oliveira Freitas, H. M. (2003). Metal hyperaccumulation in plants: Biodiversity prospecting for phytoremediation technology. *Electronic Journal of Biotechnology, 6*(3), 285–321. https://doi.org/10.2225/vol6-issue3-fulltext-6.

Raba, A., Henk, S., Meharg, A. A., & Feldmann, J. (2005). Uptake, translocation, and transformation of arsenate and arsenite in sunflower (Helianthus annuus): Formation of arsenic-phytochelatin complexes during exposure to high arsenic concentration. *New Phytologist, 168,* 551. https://doi.org/10.1111/j.1469-8137.2005.01519.x.

Rathod, P. H., Brackhage, C., Van der Meer, F. D., Müller, I., Noomen, M. F., Rossiter, D. G., et al. (2015). Spectral changes in the leaves of barley plant due to phytoremediation of metals-results from a pot study. *European Journal of Remote Sensing, 48,* 283–302. https://doi.org/10.5721/EuJRS20154816.

Rathod, P. H., Rossiter, D. G., Noomen, M. F., & Van der Meer, F. D. (2013). Proximal spectral sensing to monitor phytoremediation of metal-contaminated soils. *International Journal of Phytoremediation, 15*(5), 405–426. https://doi.org/10.1080/15226514.2012.702805.

Schwitzguébel, J. P., Nehnevajova, E., & Herzig, R. (2008). Sustainable approach to remove metals from contaminated soils: Improved phytoextraction by sunflower mutants. ID 291. In N. Kalogerakis, F. Fava & S. A. Banwart (Eds.), *E-book of abstract of the fourth European Bioremediaton conference*, Crete, Greece, September 3–6, 2008.

Slonecker, T., Haack, B., & Price, S. (2009). Spectroscopic analysis of arsenic uptake in *Pteris* ferns. *Remote Sensing, 1,* 644–675. https://doi.org/10.3390/rs1040644.

Sridhar, B. B., Han, F. X., Diehl, S. V., Monts, D. L., & Su, Y. (2007a). Monitoring the effects of arsenic and chromium accumulation in Chinese brake fern (*Pteris vittata*). *International Journal of Remote Sensing, 28*(5), 1055–1067. https://doi.org/10.1080/01431160600868466.

Sridhar, B. B., Han, F. X., Diehl, S. V., Monts, D. L., & Su, Y. (2007b). Spectral reflectance and leaf internal structure changes of barley plants due to phytoextraction of zinc and cadmium. *International Journal of Remote Sensing, 28*(5), 1041–1054. https://doi.org/10.1080/01431160500075832.

Sridhar, B. B., Witter, J. D., Wu, C., Spongberg, A. L., & Vincent, R. K. (2014). Effect of biosolids amendments on the metal and nutrient uptake and spectral characteristics of five vegetables plants. *Water, Air, and Soil Pollution, 225*(2092), 1–14. https://doi.org/10.1007/s110270-014-2092-9.

Vangronsveld, J., Herzig, R., Weyens, N., Boulet, J., Adriaensen, K., Ruttens, A., et al. (2009). Phytoremediation of contaminated soils and groundwater: Lessons from the field. *Environmental Science and Pollution Research, 16*(7), 765–794. https://doi.org/10.1007/s11356-009-0213-6.

Westad, F., & Marten, H. (2000). Variable selection in near infrared spectroscopy based on significance testing in partial least squares regression. *Journal of Near Infrared Spectroscopy, 8*(2), 117–124. https://doi.org/10.1255/jnirs.271.